

# The CP violating phase $\gamma$ from global fit of rare charmless hadronic B decays

<sup>1</sup>X.-G. He, <sup>1</sup>Y.-K. Hsiao, <sup>1</sup>J.-Q. Shi, <sup>2</sup>Y.-L. Wu and <sup>2</sup>Y.-F. Zhou

<sup>1</sup>*Department of Physics, National Taiwan University, Taipei*

<sup>2</sup>*Institute of Theoretical Physics, Academia Sinica, Beijing*

(November, 2000. Revised March, 2001)

## Abstract

We study constraints on the CP violating phase  $\gamma$  in the Kobayashi-Maskawa model using available experimental data. We first follow the conventional method to update the constraint on  $\gamma$  by performing a  $\chi^2$  analysis using data from  $|\epsilon_K|$ ,  $\Delta m_{B_{d,s}}$  and  $|V_{ub}/V_{cb}|$ . We also include the recent information on  $\sin 2\beta$  in the analysis. We obtain the best fit for  $\gamma$  to be  $66^\circ$  and the 95% C.L. allowed range to be  $42^\circ \sim 87^\circ$ . We then develop a method to carry out a  $\chi^2$  analysis based on SU(3) symmetry using data from  $B \rightarrow \pi\pi$  and  $B \rightarrow K\pi$ . We also discuss SU(3) breaking effects from model estimate. We find that present data on  $B \rightarrow \pi\pi, K\pi$  can also give some constraint on  $\gamma$  although weaker than the earlier method limited by the present experimental errors. Future improved data will provide more stringent constraint. Finally we perform a combined fit using data from  $|\epsilon_K|$ ,  $\Delta m_{B_{d,s}}$ ,  $|V_{ub}/V_{cb}|$ ,  $\sin 2\beta$  and rare charmless hadronic  $B$  decays. The combined analysis gives  $\gamma = 67^\circ$  for the best fit value and  $43^\circ \sim 87^\circ$  as the 95% C.L. allowed range. Several comments on other methods to determine  $\gamma$  based on SU(3) symmetry are also provided.

## I. INTRODUCTION

The origin of CP violation is still a mystery although it has been observed in neutral kaon mixing more than 35 years. One of the most promising model for CP violation is the model proposed by Kobayashi and Maskawa in 1973 [1]. This is now referred as the Standard Model (SM) for CP violation. In this model CP violation results from a non-removable phase  $\gamma$  in the charged current mixing matrix, the Cabbibo-Kobayashi-Maskawa (CKM) matrix [1,2],  $V_{CKM}$ . There are also other mechanisms for CP violation. To understand the origin of CP violation, it is important to study in every detail of a particular mechanism against experimental data. In this paper we carry out a study to constrain the CP violating phase in the SM using available experimental data.

The CKM matrix  $V_{CKM}$  is a  $3 \times 3$  unitary matrix and is usually written as

$$V_{CKM} = \begin{pmatrix} V_{ud} & V_{us} & V_{ub} \\ V_{cd} & V_{cs} & V_{cb} \\ V_{td} & V_{ts} & V_{tb} \end{pmatrix}. \quad (1)$$

In the literature there are several ways to parameterize the CKM matrix. The standard particle data group parameterization is given by [3]

$$V_{CKM} = \begin{pmatrix} c_{12}c_{13} & s_{12}c_{13} & s_{13}e^{-i\delta_{13}} \\ -s_{12}c_{23} - c_{12}s_{23}s_{13}e^{i\delta_{13}} & c_{12}c_{23} - s_{12}s_{23}s_{13}e^{i\delta_{13}} & s_{23}c_{13} \\ s_{12}s_{23} - c_{12}c_{23}s_{13}e^{i\delta_{13}} & -c_{12}s_{23} - s_{12}c_{23}s_{13}e^{i\delta_{13}} & c_{23}c_{13} \end{pmatrix}. \quad (2)$$

where  $s_{ij} = \sin \theta_{ij}$  and  $c_{ij} = \cos \theta_{ij}$  are the rotation angles. A non-zero value for  $\sin \delta_{13}$  violates CP. Another commonly used parameterization is the Wolfenstein parameterization [4] which expands the CKM matrix in terms of  $\lambda = |V_{us}|$  and is given by

$$V_{CKM} = \begin{pmatrix} 1 - \frac{1}{2}\lambda^2 & \lambda & A\lambda^3(\rho - i\eta) \\ -\lambda & 1 - \frac{1}{2}\lambda^2 & A\lambda^2 \\ A\lambda^3(1 - \rho - i\eta) & -A\lambda^2 & 1 \end{pmatrix} + \mathcal{O}(\lambda^4). \quad (3)$$

The parameters  $A, \rho, \eta$  are of order unity. When discussing CP violation in kaon system, it is necessary to keep higher order terms in  $\lambda$ , namely, adding  $-A^2\lambda^5(\rho + i\eta)$  and  $-A\lambda^4(\rho + i\eta)$

to  $V_{cd}$  and  $V_{ts}$ , respectively. CP violation in this parameterization is characterized by a non-zero value for  $\eta$ .

Due to the unitarity condition, one has

$$V_{ub}^*V_{ud} + V_{cb}^*V_{cd} + V_{tb}^*V_{td} = 0. \quad (4)$$

In the complex plane the above equation defines a triangle with angles  $\alpha = -\text{Arg}(V_{td}V_{tb}^*/V_{ud}V_{ub}^*)$ ,  $\beta = -\text{Arg}(V_{cd}V_{cb}^*/V_{td}V_{tb}^*)$  and  $\gamma = -\text{Arg}(V_{ud}V_{ub}^*/V_{cd}V_{cb}^*)$  as shown in Figure 1.

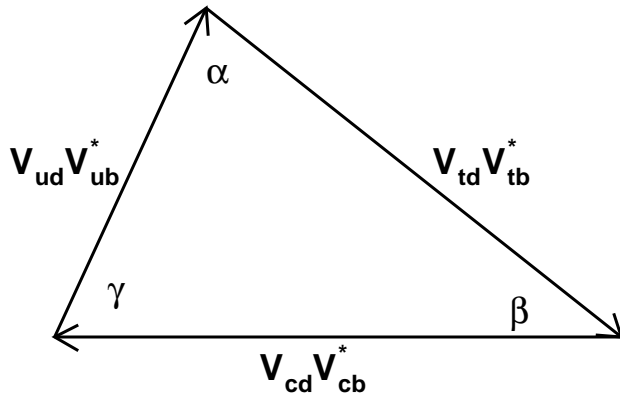


FIG. 1. The KM unitarity triangle.

To a very good approximation the phase  $\delta_{13}$  is equal to  $\gamma$ . In terms of  $\rho$  and  $\eta$ , the angles  $\alpha$ ,  $\beta$  and  $\gamma$  are given by:

$$\sin 2\alpha = \frac{2\eta(\rho^2 - \rho + \eta^2)}{((1 - \rho)^2 + \eta^2)(\rho^2 + \eta^2)}, \quad \sin 2\beta = \frac{2\eta(1 - \rho)}{(1 - \rho)^2 + \eta^2}, \quad \gamma = \tan^{-1} \frac{\eta}{\rho}. \quad (5)$$

In this paper we will concentrate on obtaining constraint on the phase  $\gamma$ . Great efforts have been made to constrain or to determine the CP violating phase  $\gamma$ . Previous studies mainly used experimental data on: i) The CP violating parameter  $\epsilon_K$  in the mixing of neutral kaons; ii) The mixing parameters  $\Delta m_{B_d}$  and  $\Delta m_{B_s}$  in  $B_{d,s} - \bar{B}_{d,s}$  systems; And iii)  $|V_{ub}/V_{cb}|$  which characterizes the strength of the charmless flavor changing and charmed flavor changing semi-leptonic  $B$  decays. The best fit value for  $\gamma$  from these considerations is around  $65^\circ$  [5,6].

During the last few years, several rare charmless hadronic  $B$  decays have been measured [7]. Some of these decays are sensitive to  $\gamma$  and therefore can be used to constrain it [8,9]. Analysis based on naive factorization approximation suggests that  $\gamma$  tends to be larger than  $90^\circ$  in conflict with the analysis mentioned earlier [8,9]. If confirmed, it is an indication of new physics beyond the SM. Of course due to uncertainties in the experimental data and theoretical calculations, it is not possible to draw a firm conclusion whether this conflict is real at present. To improve the situation, in this paper we will carry out an analysis replacing the naive factorization assumption by more general SU(3) flavor symmetry for the rare charmless hadronic decays of  $B$  to two SU(3) octet pseudoscalars  $P_1$  and  $P_2$ , that is,  $B \rightarrow PP$  decays.

SU(3) analyses for  $B$  decays have been studied by many groups and several interesting results, such as relations between different decay branching ratios, and ways to constrain and/or to determine the phase  $\gamma$ , have been obtained [10–14]. SU(3) symmetry is expected to be a good approximation for  $B$  decays. At present experimental data from  $B \rightarrow DK(\pi)$  support such an expectation [10]. However more tests are needed, especially in rare charmless hadronic  $B$  decays. Recently it has been shown that such tests can indeed be carried out for rare charmless hadronic  $B$  decays in an electroweak model independent way in the future [13]. Before this can be done, however, SU(3) symmetry can only be taken as a working hypothesis. In the rest of the paper we will study constraints which can be obtained from rare charmless hadronic  $B \rightarrow PP$  decays based on SU(3) symmetry. We will also study SU(3) breaking effects using model calculations.

The paper is arranged as follow. In section II, we will review and up date the constraint on  $\gamma$  using information from  $\epsilon_K$ ,  $\Delta m_{B_{d,s}}$  and  $|V_{ub}/V_{cb}|$ , and also information from  $\sin 2\beta$  measurement. In section III we will carry out a  $\chi^2$  analysis of  $\gamma$  using rare charmless hadronic  $B \rightarrow PP$  decay data based on SU(3) symmetry. We will also discuss SU(3) breaking effects. In section IV, we will make a combined study using results from sections II and III. And in section V, we will discuss some of the implications of the results obtained and draw our conclusions.

## II. CONSTRAINT ON $\gamma$ FROM $|\epsilon_K|$ , $\Delta M_{B_{d,s}}$ , $|V_{UB}/V_{CB}|$ AND $\sin 2\beta$

In this section we first review and up date the constraint on  $\gamma$  using experimental and theoretical information on  $\epsilon_K$ ,  $\Delta m_{B_{d,s}}$  and  $|V_{ub}/V_{cb}|$ . Such an analysis has been carried out before. The analysis in this section is an up date of the previous analyses which also serves to set up our notations for later use. We then include experimental data from  $\sin 2\beta$  measurement into the analysis to obtain the best fit value and allowed range for  $\gamma$ .

There exist quite a lot of information about the CKM matrix [3]. The value of  $V_{us}$  is known from  $K_{l3}$  decay and hyperon decays with good precision:

$$\lambda = 0.2196 \pm 0.0023.$$

The parameter  $A$  depends on  $\lambda$  and on the CKM matrix element  $|V_{cb}|$ . Using experimental data from  $B \rightarrow \bar{D}^* l^+ \nu$  and  $B \rightarrow \bar{D} l^+ \nu$  and inclusive  $b \rightarrow cl\bar{\nu}$ , analysis from LEP data obtains  $V_{cb} = 0.0402 \pm 0.0019$ , and data from CLEO obtains  $V_{cb} = 0.0404 \pm 0.0034$ . The central values of these two measurements are close to each other. In our analysis we will use the averaged value which leads to  $A = 0.835 \pm 0.034$ .

The value for  $|V_{ub}|$  has also been studied using data from  $B \rightarrow \pi l \bar{\nu}_l$ ,  $B \rightarrow \rho l \bar{\nu}_l$  and inclusive  $b \rightarrow ul\bar{\nu}_l$  with

$$|V_{ub}/V_{cb}| = \lambda \sqrt{\rho^2 + \eta^2} = 0.090 \pm 0.025 \quad (6)$$

To separately determine  $\rho$  and  $\eta$  (or  $\gamma$ ), one has to use information from other data. In the rest of this section we will carry out a  $\chi^2$  analysis using constraints from the measurements of  $|\epsilon_K|$ ,  $\Delta m_{B_{d,s}}$  and  $|V_{ub}/V_{cb}|$  along with other known experimental and theoretical information.

The parameter  $\epsilon_K$  indicates CP violation in neutral kaon mixing. The short and long lived mass eigenstates  $K_S$  and  $K_L$  of the neutral kaons can be expressed as the linear combination of weak interaction eigenstates  $K^0$  and  $\bar{K}^0$  as  $|K_S\rangle = p|K^0\rangle + q|\bar{K}^0\rangle$  and  $|K_L\rangle = p|K^0\rangle - q|\bar{K}^0\rangle$ .  $p$  and  $q$  are related to the CP violating parameter  $\epsilon_K$  in  $K_L$  decays by:

$$\frac{p}{q} = \frac{1 + \epsilon_K}{1 - \epsilon_K}. \quad (7)$$

The precise measurements of the  $K_S \rightarrow \pi\pi$  and  $K_L \rightarrow \pi\pi$  decay rates imply [3]:

$$|\epsilon_K| = (2.271 \pm 0.017) \times 10^{-3}.$$

Evaluating the so called ‘‘Box’’ diagram, one obtains

$$|\epsilon_K| = \frac{G_F^2 f_K^2 m_K m_W^2}{6\sqrt{2}\pi^2 \Delta m_K} B_K (A^2 \lambda^6 \eta) \left[ y_c (\eta_{ct} f_3(y_c, y_t) - \eta_{cc}) + \eta_{tt} y_t f_2(y_t) A^2 \lambda^4 (1 - \rho) \right]. \quad (8)$$

where  $\eta_{tt} = 0.574 \pm 0.004$ ,  $\eta_{ct} = 0.47 \pm 0.04$  and  $\eta_{cc} = 1.38 \pm 0.53$  [15] are the QCD correction factors,  $\Delta m_K = m_{K_L} - m_{K_S} = (0.5300 \pm 0.0012) \times 10^{-2} \text{ps}^{-1}$ , and  $B_K = 0.94 \pm 0.15$  [16] is the bag factor. The functions  $f_2$  and  $f_3$  of the variables  $y_t = m_t^2/m_W^2$  and  $y_c = m_c^2/m_W^2$  are given by [17]:

$$f_2(x) = \frac{1}{4} + \frac{9}{4(1-x)} - \frac{3}{2(1-x)^2} - \frac{3x^2 \ln x}{2(1-x)^3},$$

$$f_3(x, y) = \ln \frac{y}{x} - \frac{3y}{4(1-y)} \left( 1 + \frac{y \ln y}{1-y} \right). \quad (9)$$

Neutral mesons  $B_d^0$  and  $\bar{B}_d^0$  show a behavior similar to neutral kaons. The heavy and light mass eigenstates,  $B_L$  and  $B_H$ , are different from  $B_d^0$  and  $\bar{B}_d^0$  and are given by

$$|B_L\rangle = p|B_d^0\rangle + q|\bar{B}_d^0\rangle,$$

$$|B_H\rangle = p|B_d^0\rangle - q|\bar{B}_d^0\rangle. \quad (10)$$

The mass difference  $\Delta m_{B_d} = m_{B_H} - m_{B_L}$  can be measured by means of the study of the oscillations of one CP eigenstate into the other. The world average value for  $\Delta m_{B_d}$  is [18]:

$$\Delta m_{B_d} = 0.487 \pm 0.014 \text{ ps}^{-1}. \quad (11)$$

The contribution to  $\Delta m_{B_d}$  is from analogous ‘‘Box’’ diagrams as that for  $\epsilon_K$ , but with the dominant contribution from the top quark in the loop. One obtains

$$\Delta m_{B_d} = \frac{G_F^2}{6\pi^2} m_W^2 m_{B_d} (f_{B_d} \sqrt{B_{B_d}})^2 \eta_B y_t f_2(y_t) A^2 \lambda^6 [(1 - \rho)^2 + \eta^2]. \quad (12)$$

where  $f_{B_d}\sqrt{B_{B_d}} = 0.215 \pm 0.040\text{GeV}$  [19],  $\eta_B = 0.55 \pm 0.01$  [15] and the function  $f_2$  is given by Eq. (9).

$B_s^0$  and  $\bar{B}_s^0$  mesons are believed to undergo a mixing analogous to the  $B_d^0$  and  $\bar{B}_d^0$ . Their larger mass difference  $\Delta m_{B_s}$  is responsible for oscillations that are faster than the  $B_d^0$  and  $\bar{B}_d^0$  oscillation, and have thus still eluded direct observation. A lower limit has been set by the LEP, SLD and CDF collaborations, as [18]:

$$\Delta m_{B_s} > 14.9\text{ps}^{-1}(95\% \text{ C.L.}). \quad (13)$$

The expression for  $\Delta m_{B_s}$  in the SM is similar to that for  $\Delta m_{B_d}$ .  $\Delta m_{B_s}$  can be written as:

$$\Delta m_{B_s} = \Delta m_{B_d} \frac{1}{\lambda^2} \frac{m_{B_s}}{m_{B_d}} \xi^2 \frac{1}{(1-\rho)^2 + \eta^2}, \quad (14)$$

where all the theoretical uncertainties are included in a quantity  $\xi$ , which is given by [19]:

$$\xi = \frac{f_{B_s}\sqrt{B_{B_s}}}{f_{B_d}\sqrt{B_{B_d}}} = 1.14 \pm 0.06. \quad (15)$$

The  $\rho$  and  $\eta$  parameters can be determined from a fit to the experimental values of the observables described in the above. In the analysis we will adopt the strategies used in previous analysis in the literature fixing the known parameters, theoretical or experimental, to their central values if their errors were reasonably small reported in the left half of Table I. The quantities affected by large errors will be used as additional parameters of the fit, but including a constraint on their value as shown by the right half of Table I. All errors will be assumed to be Gaussian. This assumption may result in stringent constraints more than actually can be achieved because some of the errors may obey different distributions, for example those errors come from theoretical estimates may obey flat distribution. Nevertheless, the results provide a good indication for the values of the parameters involved.

To obtain the best fit values and certain confidence level allowed ranges for the relevant parameters, we perform a  $\chi^2$  analysis using the above information. The procedure for  $\chi^2$  analysis here is to minimize the following expression:

$$\begin{aligned}
\chi^2 = & \frac{(\widehat{A} - A)^2}{\sigma_A^2} + \frac{(\widehat{m}_c - m_c)^2}{\sigma_{m_c}^2} + \frac{(\widehat{m}_t - m_t)^2}{\sigma_{m_t}^2} + \frac{(\widehat{B}_K - B_K)^2}{\sigma_{B_K}^2} + \frac{(\widehat{\eta}_{cc} - \eta_{cc})^2}{\sigma_{\eta_{cc}}^2} \\
& + \frac{(\widehat{\eta}_{ct} - \eta_{ct})^2}{\sigma_{\eta_{ct}}^2} + \frac{(f_{B_d} \sqrt{\widehat{B}_{B_d}} - f_{B_d} \sqrt{B_{B_d}})^2}{\sigma_{f_{B_d} \sqrt{B_{B_d}}}^2} + \frac{(\widehat{\xi} - \xi)^2}{\sigma_{\xi}^2} + \frac{(\frac{|V_{ub}|}{|V_{cb}|} - \frac{|V_{ub}|}{|V_{cb}|})^2}{\sigma_{\frac{|V_{ub}|}{|V_{cb}|}}^2} \\
& + \frac{(|\widehat{\epsilon}_K| - |\epsilon_K|)^2}{\sigma_{|\epsilon_K|}^2} + \frac{(\Delta \widehat{m}_{B_d} - \Delta m_{B_d})^2}{\sigma_{\Delta m_{B_d}}^2} + \chi^2(A(\Delta m_{B_s}), \sigma_A(\Delta m_{B_s})). \tag{16}
\end{aligned}$$

The symbols with a hat represent the reference values measured or calculated for given physical quantities, as listed in Table I, while the corresponding  $\sigma$  are their errors. The parameters of the fit are  $\rho$ ,  $\eta$ ,  $A$ ,  $m_c$ ,  $m_t$ ,  $B_K$ ,  $\eta_{ct}$ ,  $\eta_{cc}$ ,  $f_{B_d} \sqrt{B_{B_d}}$  and  $\xi$ .

TABLE I. Input parameters for  $\chi^2$  analysis using data from  $\epsilon_K$ ,  $\Delta m_{B_{d,s}}$  and  $|V_{ub}/V_{cb}|$ .

Fixed values		Varied parameters	
$\lambda = 0.2196 \pm 0.0023$	[3]	$A = 0.835 \pm 0.034$	[3]
$G_F = (1.16639 \pm 0.00001) \times 10^{-5} \text{ GeV}^{-2}$	[3]	$\eta_{ct} = 0.47 \pm 0.04$	[15]
$f_K = 0.1598 \pm 0.0015 \text{ GeV}$	[3]	$\eta_{cc} = 1.38 \pm 0.53$	[15]
$\Delta m_K = (0.5300 \pm 0.0012) \times 10^{-2} \text{ ps}^{-1}$	[3]	$\overline{m}_c(m_c) = 1.25 \pm 0.10 \text{ GeV}$	[3]
$m_K = 0.497672 \pm 0.000031 \text{ GeV}$	[3]	$\overline{m}_t(m_t) = 165.0 \pm 5.0 \text{ GeV}$	[3]
$m_W = 80.419 \pm 0.056 \text{ GeV}$	[3]	$f_{B_d} \sqrt{B_{B_d}} = 0.215 \pm 0.040 \text{ GeV}$	[16]
$m_{B_d} = 5.2794 \pm 0.0005 \text{ GeV}$	[3]	$B_K = 0.94 \pm 0.15$	[16]
$m_{B_s} = 5.3696 \pm 0.0024 \text{ GeV}$	[3]	$\xi = 1.14 \pm 0.06$	[16]
$\eta_{tt} = 0.574 \pm 0.004$	[15]	$ \epsilon_K  = (2.271 \pm 0.017) \times 10^{-3}$	[3]
$\eta_B = 0.55 \pm 0.01$	[15]	$\Delta m_{B_d} = 0.487 \pm 0.014 \text{ ps}^{-1}$	[18]
		$ V_{ub}/V_{cb}  = 0.090 \pm 0.025$	[3]

The inclusion of the  $\Delta m_{B_s}$  data needs some explanation. The experimental data consists of measured values of  $\mathcal{A}(\Delta m_{B_s})$  and  $\sigma_{\mathcal{A}}(\Delta m_{B_s})$  for various values of  $\Delta m_{B_s}$  plot in Figure 2. To include this data in the fit, for each set of free parameters ( $A, \rho, \eta, \xi$ ) we calculate the value of  $\Delta m_{B_s}$  and find the corresponding experimental values of  $\mathcal{A}$  and  $\sigma_{\mathcal{A}}$  in Figure 2. A



nonzero value of  $\Delta m_{B_s}$  implies that there is  $B_s^0 - \bar{B}_s^0$  mixing, if observed one should have  $\mathcal{A} = 1$  and otherwise  $\mathcal{A} = 0$  [20]. We follow Ref. [6] to add to the total  $\chi^2$  in Eq. (16) a  $\Delta\chi^2$  for the corresponding set of  $(A, \rho, \eta, \xi)$ ,

$$\Delta\chi^2 = \chi^2(\mathcal{A}(\Delta m_{B_s}), \sigma_{\mathcal{A}}(\Delta m_{B_s})) = \left(\frac{\mathcal{A} - 1}{\sigma_{\mathcal{A}}}\right)^2. \quad (17)$$

$\text{Exp}[-\Delta\chi^2/2]$  is an indication of how likely a mixing with a given  $\Delta m_{B_s}$  was measured by experiment. The sign of the deviation  $\mathcal{A} - 1$  should also be carefully treated. Naively the expression of  $\Delta\chi^2$  implies that a lower probability is attributed to the  $\Delta m_{B_s}$  values with  $\mathcal{A} > 1$  with respect to  $\Delta m_{B_s}$  values having  $\mathcal{A} = 1$ . To avoid this undesired behavior, we follow Ref. [6] to set  $\mathcal{A}$  to unity for the range with  $\mathcal{A}$  larger than one in Fig. 2.

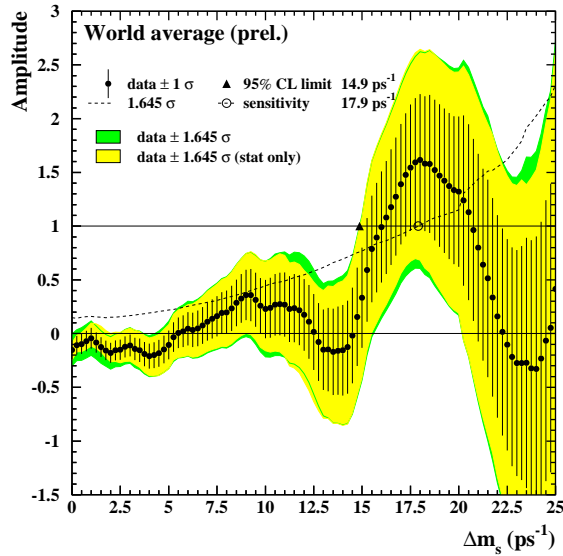


FIG. 2. Experimental data on  $\Delta m_{B_s}$  [17].

After  $\rho$  and  $\eta$  are determined it is easy to obtain the values of the angles in the unitarity triangle using relations in Eq. (5). The best fit values and the allowed regions in the  $\rho - \eta$  plane are shown in Figure 3. The best fit values and their 68% C.L. errors are

$$\begin{aligned} \rho &= 0.18_{-0.09}^{+0.11}, & \eta &= 0.34_{-0.06}^{+0.07}, \\ \sin 2\alpha &= -0.19_{-0.42}^{+0.37}, & \sin 2\beta &= 0.70_{-0.09}^{+0.14}, & \gamma &= 62_{-13}^{+12} \text{ degrees}. \end{aligned} \quad (18)$$

The 95% C.L. allowed regions for the above quantities are expressed as:

$$\begin{aligned}
0.03 < \rho < 0.38, \quad 0.23 < \eta < 0.50, \\
-0.85 < \sin 2\alpha < 0.42, \quad 0.49 < \sin 2\beta < 0.94, \quad 39^\circ < \gamma < 84^\circ.
\end{aligned}
\tag{19}$$

These results agree with previous analyses [5].

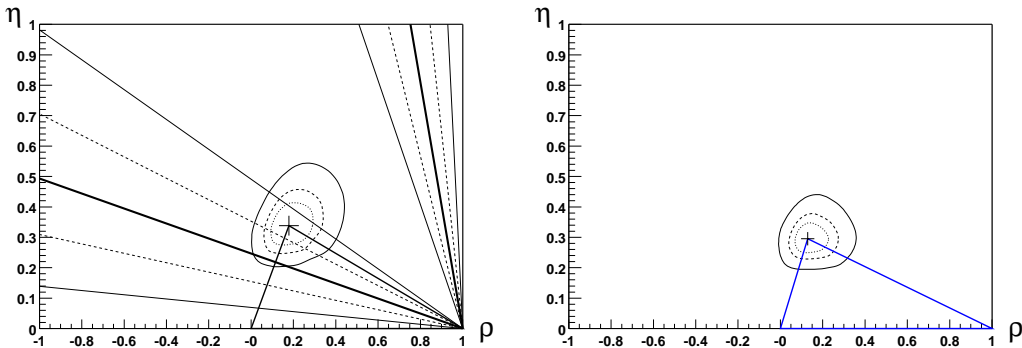


FIG. 3. Constraints on  $\rho$  and  $\eta$  using data from  $|\epsilon_K|$ ,  $\Delta m_{B_{d,s}}$  and  $|V_{ub}/V_{cb}|$ , and  $\sin 2\beta$ . In the figure on the left, only  $|\epsilon_K|$ ,  $\Delta m_{B_{d,s}}$  and  $|V_{ub}/V_{cb}|$  are used. The best fit value is indicated by the “+” symbol. The region in the dotted curve corresponds to  $\chi^2 - \chi_{min}^2 = 1$  allowed region which is at the 39% C.L.. The 68% C.L. allowed region is within the dashed curve and the 95% C.L. allowed region is within the solid curve. The straight ray lines are the results for direct measurement of  $\sin 2\beta$ . The thick solid lines are for the central value of  $\sin 2\beta$ . There are two allowed regions. The region outside the two thin solid straight lines for each allowed region are excluded by the  $\sin 2\beta$  measurement at 95% C.L.. The 68% C.L. allowed regions are between the dashed lines. The figure on the right is a fit with  $\sin 2\beta$  data also included in the  $\chi^2$ .

The solid line in Figure 4 is a plot of the minimal  $\chi^2$  as a function of  $\gamma$  for the fit using  $|\epsilon_K|$ ,  $\Delta m_{B_{d,s}}$  and  $|V_{ub}/V_{cb}|$ . It is clear that  $\chi^2$  changes with  $\gamma$  dramatically. When going away from the minimal,  $\chi^2$  raises rapidly indicating a good determination of  $\gamma$ .

There are also direct measurements of  $\sin 2\beta$  by several groups from the time dependent CP asymmetry in  $B \rightarrow J/\psi K_S$ . In the SM this asymmetry is given by

$$a(t) = \frac{\Gamma(\bar{B}^0(t) \rightarrow J/\psi K_S) - \Gamma(B^0(t) \rightarrow J/\psi K_S)}{\Gamma(\bar{B}^0(t) \rightarrow J/\psi K_S) + \Gamma(B^0(t) \rightarrow J/\psi K_S)} = -\sin 2\beta \sin(\Delta m_{B_d} t).
\tag{20}$$

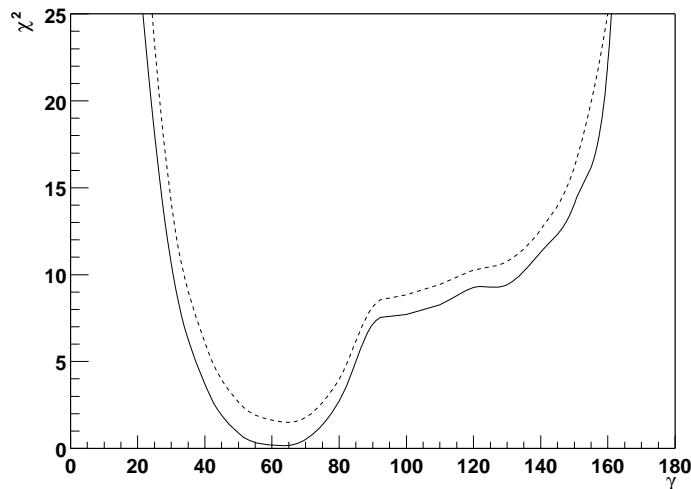


FIG. 4. The solid line is the  $\chi^2$  as a function of  $\gamma$  using data from  $|\epsilon_K|$ ,  $\Delta m_{B_{d,s}}$  and  $|V_{ub}/V_{cb}|$ . The dashed line is the  $\chi^2$  as a function of  $\gamma$  with  $\sin 2\beta$  data included in the fit.

The values measured by different groups are,

$$\sin 2\beta = \begin{cases} 0.34 \pm 0.20 \pm 0.05; & \text{BaBar [21]} \\ 0.58^{+0.32+0.09}_{-0.34-0.10}; & \text{Belle [21]} \\ 0.79^{+0.41}_{-0.44}; & \text{CDF [22]} \\ 0.84^{+0.82}_{-1.04} \pm 0.16 & \text{ALEPH [23]} \end{cases} \quad (21)$$

The averaged value is  $\sin 2\beta = 0.46 \pm 0.16$ .

For a given  $\sin 2\beta$  there are, in general, four solutions for  $\gamma$  with two of them having negative  $\eta$  and another two having positive  $\eta$ . To determine which one of them is the right solution, one has to use other information. Using the information from our previous fit, we can rule out some of the solutions. The allowed ranges for  $\rho$  and  $\eta$  from the averaged value for  $\sin 2\beta$  is shown in the figure on the left in Fig. 3 by the straight ray lines. Since the fit from  $|\epsilon_K|$ ,  $\Delta m_{B_{d,s}}$  and  $|V_{ub}/V_{cb}|$  determines  $\eta > 0$ , only solutions with  $\eta > 0$  are allowed. It is clear that one of the values for  $\rho$  and  $\eta$  determined from  $\sin 2\beta$  measurement can be consistent with the fitting results in Eqs. (18) and (19).

It is interesting to note that  $\sin 2\beta$  data can eliminate a large allowed range in the  $\rho$  vs.  $\eta$  plane at the 95% C.L. level. One can also include the measured  $\sin 2\beta$  into the  $\chi^2$  analysis. The results are shown in the figure on the right in Fig.3. The  $\chi^2$  as a function of  $\gamma$  is shown

by the dashed line in Fig. 4. The best fit values and their 68% C.L. errors are given by:

$$\begin{aligned} \rho &= 0.13_{-0.06}^{+0.10}, \quad \eta = 0.30_{-0.05}^{+0.05}, \\ \sin 2\alpha &= -0.19_{-0.44}^{+0.35}, \quad \sin 2\beta = 0.61_{-0.07}^{+0.09}, \quad \gamma = 66_{-14}^{+10}. \end{aligned} \quad (22)$$

And the 95% C.L. allowed regions for the above quantities are:

$$\begin{aligned} 0.01 < \rho < 0.30, \quad 0.21 < \eta < 0.41, \\ -0.88 < \sin 2\alpha < 0.45, \quad 0.40 < \sin 2\beta < 0.80, \quad 42^\circ < \gamma < 87^\circ. \end{aligned} \quad (23)$$

### III. DETERMINATION OF $\gamma$ FROM CHARMLESS HADRONIC $B$ DECAYS

In this section we study how the phase  $\gamma$  can be constrained from experimental data on  $B \rightarrow PP$  decays, based on flavor SU(3) symmetry consideration.

#### A. The Quark Level Effective Hamiltonian

The quark level effective Hamiltonian up to one loop level in electroweak interaction for charmless hadronic  $B$  decays, including QCD corrections to the matrix elements, can be written as

$$H_{eff}^q = \frac{G_F}{\sqrt{2}} [V_{ub}V_{uq}^*(c_1O_1 + c_2O_2) - \sum_{i=3}^{11} (V_{ub}V_{uq}^*c_i^{uc} + V_{tb}V_{tq}^*c_i^{tc})O_i]. \quad (24)$$

The coefficients  $c_{1,2}$  and  $c_i^{jk} = c_i^j - c_i^k$ , with  $j$  indicates the internal quark, are the Wilson Coefficients (WC). These WC's have been evaluated by several groups [24], with  $|c_{1,2}| \gg |c_i^j|$ . In the above the factor  $V_{cb}V_{cq}^*$  has been eliminated using the unitarity property of the CKM matrix. The operators  $O_i$  are defined as [24],

$$\begin{aligned} O_1 &= (\bar{q}_i u_j)_{V-A} (\bar{u}_j b_i)_{V-A}, & O_2 &= (\bar{q} u)_{V-A} (\bar{u} b)_{V-A}, \\ O_{3,5} &= (\bar{q} b)_{V-A} \sum_{q'} (\bar{q}' q')_{V\mp A}, & O_{4,6} &= (\bar{q}_i b_j)_{V-A} \sum_{q'} (\bar{q}'_j q'_i)_{V\mp A}, \\ O_{7,9} &= \frac{3}{2} (\bar{q} b)_{V-A} \sum_{q'} e_{q'} (\bar{q}' q')_{V\pm A}, & O_{8,10} &= \frac{3}{2} (\bar{q}_i b_j)_{V-A} \sum_{q'} e_{q'} (\bar{q}'_j q'_i)_{V\pm A}, \\ O_{11} &= \frac{g_s}{8\pi^2} \bar{q} \sigma_{\mu\nu} G^{\mu\nu} (1 + \gamma_5) b. \end{aligned} \quad (25)$$

where  $(\bar{q}_1 q_2)_{V-A} = \bar{q}_1 \gamma_\mu (1 - \gamma_5) q_2$ ,  $G^{\mu\nu}$  is the field strengths of the gluon, respectively. We have neglected the photonic dipole penguin term whose contribution to hadronic charmless  $B$  decays is small. The usual tree-level W-exchange contribution in the effective Hamiltonian corresponds to  $O_2$ .  $O_1$  emerges due to the QCD corrections. The operators  $O_{3,4,5,6}$  are from the QCD-penguin diagrams. The operators  $O_{7,\dots}, O_{10}$  arise from the electroweak-penguin diagrams.  $O_{11}$  is the gluonic dipole penguin operator.

The WC's at  $\mu = 5$  GeV with  $\alpha_s(m_Z) = 0.118$ , in the regularization independent scheme in Ref. [25] are

$$\begin{aligned}
c_1 &= -0.313 , & c_2 &= 1.150 , \\
c_3^t &= 0.017 , & c_4^t &= -0.037 , \\
c_5^t &= 0.010 , & c_6^t &= -0.046 , \\
c_7^t &= -0.001\alpha_{em} , & c_8^t &= 0.049\alpha_{em} , \\
c_9^t &= -1.321\alpha_{em} , & c_{10}^t &= 0.267\alpha_{em} \\
c_{11}^t &= -0.143 .
\end{aligned} \tag{26}$$

where  $\alpha_{em} = 1/128$ .  $c_i^{c,u}$  are given in Ref. [25]

### B. SU(3) Structure of the Effective Hamiltonian

To obtain  $B$  decay amplitudes, one has to calculate hadronic matrix elements from quark operators. At present there is no reliable methods to calculate these matrix elements although simple factorization calculations provide some reasonable results for some decays, but not all of them [26]. It motivates us to carry out model independent analysis by studying properties of the effective Hamiltonian under SU(3) flavor symmetry and use them to obtain information about related decays.

In general the decay amplitudes for  $B \rightarrow PP$  can be written as

$$A(B \rightarrow PP) = \langle P P | H_{eff}^q | B \rangle = \frac{G_F}{\sqrt{2}} [V_{ub} V_{uq}^* T(q) + V_{tb} V_{tq}^* P(q)] , \tag{27}$$

where  $T(q)$  contains contributions from the *tree* operators  $O_{1,2}$  as well as *penguin* operators  $O_{3-11}$  due to charm and up quark loop corrections to the matrix elements, while  $P(q)$

contains contributions purely from *penguin* due to top and charm quarks in loops. The amplitude  $T$  in Eqs. (27) is usually called the “tree” amplitude which will also be referred to later on in the paper. One should, however, keep in mind that it contains the usual tree current-current contributions proportional to  $c_{1,2}$  and also the u and c penguin contributions proportional to  $c_i^{uc}$  with  $i = 3 - 11$ . Also, in general, it contains long distance contributions corresponding to internal u and c generated intermediate hadron states. In our later analysis, we do not distinguish between the tree and the penguin contributions in the amplitude  $T$ .

The relative strength of the amplitudes  $T$  and  $P$  is predominantly determined by their corresponding WC’s in the effective Hamiltonian. For  $\Delta S = 0$  charmless decays, the dominant contributions are due to the tree operators  $O_{1,2}$  and the penguin operators are suppressed by smaller WC’s. Whereas for  $\Delta S = -1$  decays, because the penguin contributions are enhanced by a factor of  $V_{tb}V_{ts}^*/V_{ub}V_{us}^* \approx 50$  [3] compared with the tree contributions, penguin effects dominate the decay amplitudes. In this case the electroweak penguins can also play a very important role [27].

The operators  $O_{1,2}$ ,  $O_{3-6,11}$ , and  $O_{7-10}$  transform under SU(3) symmetry as  $\bar{3} + \bar{3}' + 6 + \bar{15}$ ,  $\bar{3}$ , and  $\bar{3} + \bar{3}' + 6 + \bar{15}$ , respectively. We now give details for the decomposition under SU(3) for some operators. For  $\Delta S = 0$  decays,  $O_2$  can be written, omitting the Lorentz-Dirac structure, as [13]:

$$\begin{aligned}
O_2 &= -\frac{1}{8}\{(\bar{u}u)(\bar{d}b) + (\bar{d}d)(\bar{d}b) + (\bar{s}s)(\bar{d}b)\}_{\bar{3}} \\
&+ \frac{3}{8}\{(\bar{d}u)(\bar{u}b) + (\bar{d}d)(\bar{d}b) + (\bar{d}s)(\bar{s}b)\}_{\bar{3}'} \\
&- \frac{1}{4}\{(\bar{u}u)(\bar{d}b) - (\bar{d}u)(\bar{u}b) + (\bar{d}s)(\bar{s}b) - (\bar{s}s)(\bar{d}b)\}_6 \\
&+ \frac{1}{8}\{3(\bar{u}u)(\bar{d}b) + 3(\bar{d}u)(\bar{u}b) - (\bar{d}s)(\bar{s}b) - (\bar{s}s)(\bar{d}b) - 2(\bar{d}d)(\bar{d}b)\}_{\bar{15}} \\
&= -\frac{1}{8}H(\bar{3}) + \frac{3}{8}H(\bar{3}') - \frac{1}{4}H(6) + \frac{1}{8}H(\bar{15})
\end{aligned} \tag{28}$$

The  $\bar{3}$ , 6 and  $\bar{15}$  indicate the SU(3) irreducible representations. The non-zero entries of the matrices  $H(i)$  in flavor space are [10]:

$$H(\bar{3})^2 = H(\bar{3}')^2 = 1, \quad H(6)_1^{12} = H(6)_3^{23} = 1, \quad H(6)_1^{21} = H(6)_3^{32} = -1,$$

$$H(\overline{15})_1^{12} = H(\overline{15})_1^{21} = 3, \quad H(\overline{15})_2^{22} = -2, \quad H(\overline{15})_3^{32} = H(\overline{15})_3^{23} = -1. \quad (29)$$

Here  $1 = u$ ,  $2 = d$  and  $3 = s$  with the upper indices indicating anti-quarks and the lower ones indicating quarks.

For  $\Delta S = 1$  decays, one has

$$\begin{aligned} O_2 &= -\frac{1}{8}\{(\bar{u}u)(\bar{s}b) + (\bar{d}d)(\bar{s}b) + (\bar{s}s)(\bar{s}b)\}_{\bar{3}} \\ &\quad + \frac{3}{8}\{(\bar{s}u)(\bar{u}b) + (\bar{s}d)(\bar{d}b) + (\bar{s}s)(\bar{s}b)\}_{\bar{3}'} \\ &\quad - \frac{1}{4}\{(\bar{u}u)(\bar{s}b) - (\bar{s}u)(\bar{u}b) + (\bar{s}d)(\bar{d}b) - (\bar{d}d)(\bar{s}b)\}_6 \\ &\quad + \frac{1}{8}\{3(\bar{u}u)(\bar{s}b) + 3(\bar{s}u)(\bar{u}b) - (\bar{s}s)(\bar{s}b) - (\bar{s}d)(\bar{d}b) - 2(\bar{d}d)(\bar{s}b)\}_{\overline{15}} \\ &= -\frac{1}{8}H(\bar{3}) + \frac{3}{8}H(\bar{3}') - \frac{1}{4}H(6) + \frac{1}{8}H(\overline{15}) \end{aligned} \quad (30)$$

The non-zero entries are [10]:

$$\begin{aligned} H(\bar{3})^3 &= H(\bar{3}')^3 = 1, \quad H(6)_1^{13} = H(6)_2^{32} = 1, \quad H(6)_1^{31} = H(6)_2^{23} = -1, \\ H(\overline{15})_1^{13} &= H(\overline{15})_1^{31} = 3, \quad H(\overline{15})_3^{33} = -2, \quad H(\overline{15})_2^{32} = H(\overline{15})_2^{23} = -1. \end{aligned} \quad (31)$$

For  $\Delta S = 0$ , the operators  $O_{1,2}$ ,  $O_{3-6}$ , and  $O_{7-10}$  can be decomposed as

$$\begin{aligned} O_1 &= \frac{3}{8}\mathcal{O}_{\bar{3}} - \frac{1}{8}\mathcal{O}_{\bar{3}'} + \frac{1}{4}\mathcal{O}_6 + \frac{1}{8}\mathcal{O}_{\overline{15}}, \\ O_2 &= -\frac{1}{8}\mathcal{O}_{\bar{3}} + \frac{3}{8}\mathcal{O}_{\bar{3}'} - \frac{1}{4}\mathcal{O}_6 + \frac{1}{8}\mathcal{O}_{\overline{15}}, \\ O_3 &= \mathcal{O}_{\bar{3}}, \quad O_4 = \mathcal{O}_{\bar{3}'}, \\ O_9 &= \frac{3}{2}O_1 - \frac{1}{2}O_3, \quad O_{10} = \frac{3}{2}O_2 - \frac{1}{2}O_4. \end{aligned} \quad (32)$$

where

$$\begin{aligned} \mathcal{O}_{\bar{3}} &= (\bar{u}u)_{V-A}(\bar{d}b)_{V-A} + (\bar{d}d)_{V-A}(\bar{d}b)_{V-A} + (\bar{s}s)_{V-A}(\bar{d}b)_{V-A}, \\ \mathcal{O}_{\bar{3}'} &= (\bar{d}u)_{V-A}(\bar{u}b)_{V-A} + (\bar{d}d)_{V-A}(\bar{d}b)_{V-A} + (\bar{d}s)_{V-A}(\bar{s}b)_{V-A}, \\ \mathcal{O}_6 &= (\bar{u}u)_{V-A}(\bar{d}b)_{V-A} - (\bar{d}u)_{V-A}(\bar{u}b)_{V-A} \\ &\quad + (\bar{d}s)_{V-A}(\bar{s}b)_{V-A} - (\bar{s}s)_{V-A}(\bar{d}b)_{V-A}, \\ \mathcal{O}_{\overline{15}} &= 3(\bar{u}u)_{V-A}(\bar{d}b)_{V-A} + 3(\bar{d}u)_{V-A}(\bar{u}b)_{V-A} - (\bar{d}s)_{V-A}(\bar{s}b)_{V-A} \\ &\quad - (\bar{s}s)_{V-A}(\bar{d}b)_{V-A} - 2(\bar{d}d)_{V-A}(\bar{d}b)_{V-A}. \end{aligned} \quad (33)$$

The operators  $O_5$  and  $O_6$  have same SU(3) structure as  $O_3$  and  $O_4$  but different Lorentz-Dirac structures.  $O_7, O_8$  have the same SU(3) structure as  $O_9, O_{10}$ , but again have different Lorentz-Dirac structures. Similarly one can obtain the decomposition of the operators for  $\Delta S = 1$  case.

Since we are only concerned with flavor structure in SU(3), operators with different Lorentz-Dirac structures and different color structures can be grouped together according to their flavor SU(3) representations without affect the results. As long as flavor structure is concerned, the effective Hamiltonian contains only  $\bar{3}$ , 6 and  $\bar{15}$ . These properties enable us to write the decay amplitudes for  $B \rightarrow PP$  in only a few SU(3) invariant amplitudes.

### C. SU(3) Decay Amplitudes for $B \rightarrow PP$ Decays

We will use  $B_i = (B_u, B_d, B_s) = (B^-, \bar{B}^0, \bar{B}_s^0)$  to indicate the SU(3) triplet for the three  $B$ -mesons, and  $M$  to indicate the pseudoscalar octet  $M$  which contains one of the  $P$  in the final state with

$$M = \begin{pmatrix} \frac{\pi^0}{\sqrt{2}} + \frac{\eta_8}{\sqrt{6}} & \pi^+ & K^+ \\ \pi^- & -\frac{\pi^0}{\sqrt{2}} + \frac{\eta_8}{\sqrt{6}} & K^0 \\ K^- & \bar{K}^0 & -2\frac{\eta_8}{\sqrt{6}} \end{pmatrix}. \quad (34)$$

One can write the  $T$  amplitude for  $B \rightarrow PP$  as [10]

$$\begin{aligned} T &= A_3^T B_i H(\bar{3})^i (M_l^k M_k^l) + C_3^T B_i M_k^i M_j^k H(\bar{3})^j \\ &+ A_6^T B_i H(6)_k^{ij} M_j^l M_l^k + C_6^T B_i M_j^i H(6)_l^{jk} M_k^l \\ &+ A_{15}^T B_i H(\bar{15})_k^{ij} M_j^l M_l^k + C_{15}^T B_i M_j^i H(\bar{15})_l^{jk} M_k^l, \end{aligned} \quad (35)$$

due to the anti-symmetric nature in exchanging the upper two indices of  $H_k^{ij}(6)$ , and the symmetric structure of the two mesons in the final states,  $C_6 - A_6$  always appear together [10]. We will just use  $C_6$  to indicate this combination. There are 5 complex independent SU(3) invariant amplitudes. The results for each individual  $B$  decay mode are shown in Table



TABLE II. SU(3) decay amplitudes for  $B \rightarrow PP$  decays.

$\Delta S = 0$	$\Delta S = -1$
$T_{\pi^-\pi^0}^{Bu}(d) = \frac{8}{\sqrt{2}}C_{15}^T,$	$T_{\pi^-\bar{K}^0}^{Bu}(s) = C_3^T - C_6^T + 3A_{15}^T - C_{15}^T,$
$T_{\pi^-\eta_8}^{Bu}(d) = \frac{2}{\sqrt{6}}(C_3^T - C_6^T + 3A_{15}^T + 3C_{15}^T),$	$T_{\pi^0K^-}^{Bu}(s) = \frac{1}{\sqrt{2}}(C_3^T - C_6^T + 3A_{15}^T + 7C_{15}^T),$
$T_{K^-\bar{K}^0}^{Bu}(d) = C_3^T - C_6^T + 3A_{15}^T - C_{15}^T,$	$T_{\eta_8K^-}^{Bu}(s) = \frac{1}{\sqrt{6}}(-C_3^T + C_6^T - 3A_{15}^T + 9C_{15}^T),$
$T_{\pi^+\pi^-}^{Ba}(d) = 2A_3^T + C_3^T + C_6^T + A_{15}^T + 3C_{15}^T,$	$T_{\pi^+K^-}^{Ba}(s) = C_3^T + C_6^T - A_{15}^T + 3C_{15}^T,$
$T_{\pi^0\pi^0}^{Ba}(d) = \frac{1}{\sqrt{2}}(2A_3^T + C_3^T + C_6^T + A_{15}^T - 5C_{15}^T),$	$T_{\pi^0\bar{K}^0}^{Ba}(s) = -\frac{1}{\sqrt{2}}(C_3^T + C_6^T - A_{15}^T - 5C_{15}^T),$
$T_{K^-\bar{K}^+}^{Ba}(d) = 2(A_3^T + A_{15}^T),$	$T_{\eta_8\bar{K}^0}^{Ba}(s) = -\frac{1}{\sqrt{6}}(C_3^T + C_6^T - A_{15}^T - 5C_{15}^T),$
$T_{K^0\bar{K}^0}^{Ba}(d) = 2A_3^T + C_3^T - C_6^T - 3A_{15}^T - C_{15}^T,$	$T_{\pi^+\pi^-}^{Bs}(s) = 2(A_3^T + A_{15}^T),$
$T_{\pi^0\eta_8}^{Ba}(d) = \frac{1}{\sqrt{3}}(-C_3^T + C_6^T + 5A_{15}^T + C_{15}^T),$	$T_{\pi^0\pi^0}^{Bs}(s) = \sqrt{2}(A_3^T + A_{15}^T),$
$T_{\eta_8\eta_8}^{Ba}(d) = \frac{1}{\sqrt{2}}(2A_3^T + \frac{1}{3}C_3^T - C_6^T - A_{15}^T + C_{15}^T),$	$T_{K^+K^-}^{Bs}(s) = 2A_3^T + C_3^T + C_6^T + A_{15}^T + 3C_{15}^T,$
$T_{K^+\pi^-}^{Bs}(d) = C_3^T + C_6^T - A_{15}^T + 3C_{15}^T,$	$T_{K^0\bar{K}^0}^{Bs}(s) = 2A_3^T + C_3^T - C_6^T - 3A_{15}^T - C_{15}^T,$
$T_{K^0\pi^0}^{Bs}(d) = -\frac{1}{\sqrt{2}}(C_3^T + C_6^T - A_{15}^T - 5C_{15}^T),$	$T_{\pi^0\eta_8}^{Bs}(s) = \frac{2}{\sqrt{3}}(C_6^T + 2A_{15}^T - 2C_{15}^T),$
$T_{K^0\eta_8}^{Bs}(d) = -\frac{1}{\sqrt{6}}(C_3^T + C_6^T - A_{15}^T - 5C_{15}^T),$	$T_{\eta_8\eta_8}^{Bs}(s) = \sqrt{2}(A_3^T + \frac{2}{3}C_3^T - A_{15}^T - 2C_{15}^T).$

II. Similarly one can write down the expressions for the penguin induced decay amplitudes  $P$ .

Since there are both tree and penguin amplitudes  $C_i^T$ ,  $A_i^T$  and  $C_i^P$ ,  $A_i^P$ , there in general, 10 complex hadronic parameters (20 real parameters). However simplifications can be made by noticing that  $c_{7,8}$  are very small compared with other Wilson Coefficients, their contributions can be neglected to a very good precision. In that case, from Eq. (32), we obtain

$$\begin{aligned}
 C_6^P(A_6^P) &= -\frac{3}{2} \frac{c_9^{tc} - c_{10}^{tc}}{c_1 - c_2 - 3(c_9^{uc} - c_{10}^{uc})/2} C_6^T(A_6^T) \approx -\frac{3}{2} \frac{c_9^t - c_{10}^t}{c_1 - c_2} C_6^T(A_6^T), \\
 C_{15}^P(A_{15}^P) &= -\frac{3}{2} \frac{c_9^{tc} + c_{10}^{tc}}{c_1 + c_2 - 3(c_9^{uc} + c_{10}^{uc})/2} C_{15}^T(A_{15}^T) \approx -\frac{3}{2} \frac{c_9^t + c_{10}^t}{c_1 + c_2} C_{15}^T(A_{15}^T).
 \end{aligned} \tag{36}$$

We have checked that the approximation signs in the above are good to  $10^{-4}$ .

At leading order QCD correction, the above relations are renormalization scale inde-

pendent, and therefore to this order the coefficients  $C_i$  and  $A_i$  are also so. This can be seen from the fact that when keeping terms which mix only between  $O_1(O_9)$  and  $O_2(O_{10})$ , the dominant QCD correction gives:  $c_{1(9)}(\mu) + c_{2(10)}(\mu) = \eta^{2/\beta}[c_{1(9)}(m_W) + c_{2(10)}(m_W)]$  and  $c_{1(9)}(\mu) - c_{2(10)}(\mu) = \eta^{-4/\beta}[c_{1(9)}(m_W) - c_{2(10)}(m_W)]$ . Here  $c_{1,2,9,10}(m_W)$  are the initial values for the WC's at the W mass scale with  $c_{1(10)}(m_W) = 0$ ,  $\eta = \alpha_s(m_W)/\alpha_s(\mu)$  and  $\beta = 11 - 2f/3$  ( $f$  is the number of quark flavors with mass smaller than  $\mu$ ). These relations lead to  $(c_9(\mu) \pm c_{10}(\mu))/(c_1(\mu) \pm c_2(\mu)) = \pm c_9(m_W)/c_2(m_W)$  independent of  $\mu$ . Mixings with other operators and higher order corrections introduce dependence on renormalization schemes. We have checked with different renormalization schemes and find that numerically the changes are less than 15% for different schemes. Although the changes are not sizable, there are scheme dependence. The total decay amplitudes are not renormalization scheme dependent, therefore the hadronic matrix elements determined depend on the renormalization scheme used to determine the ratios,  $(c_9 \pm c_{10})/(c_1 \pm c_2)$ . One should consistently use the same scheme.

Using relations in Eq.(36), one finds that there are less independent parameters which we choose them to be,  $C_3^{T,P}(A_3^{T,P})$ ,  $C_6^T$ , and  $C_{15}^T(A_{15}^T)$ . Using the fact that an overall phase can be removed without loss of generality, we will set  $C_3^P$  to be real. There are in fact only 13 real independent parameters for  $B \rightarrow PP$  in the SM.

One can further reduce the parameters with some dynamic considerations. To this end we note that the amplitudes  $A_i$  correspond to annihilation contributions, as can be seen from Eq.(35) where  $B_i$  mesons are contracted with one of the index in  $H(j)$ , are small compared with the amplitudes  $C_i$  from model calculations and are often neglected in factorization calculations [8,26]. Neglecting all annihilation contributions, we then have just 7 independent hadronic parameters in the amplitudes

$$C_3^P, C_3^T e^{i\delta_3}, C_6^T e^{i\delta_6}, C_{15}^T e^{i\delta_{15}}. \quad (37)$$

The phases in the above are defined in such a way that all  $C_i^{T,P}$  are real positive numbers.

We will make the assumption that annihilation amplitudes are negligibly small in our

later analysis and leave the verification of this assumption for future experimental data. We point out that this assumption can be tested using  $B_d \rightarrow K^-K^+$ ,  $B_s \rightarrow \pi^+\pi^-$ ,  $\pi^0\pi^0$  in  $B \rightarrow PP$  decays, because these decays have only annihilation contributions as can be seen from Table 2 [12,13].

#### D. Constraint on $\gamma$ from $B \rightarrow PP$ Decays

We are now ready to carry out a  $\chi^2$  analysis using data from  $B \rightarrow \pi\pi$  and  $B \rightarrow K\pi$ . The experimental data to be used are shown in Table III.

In general the errors for the experimental data in Table III are correlated. Due to the lack of knowledge of the error correlation from experiments, in our analysis, for simplicity, we take them to be uncorrelated and assume the errors obey Gaussian distribution taking the larger one between  $\sigma_+$  and  $\sigma_-$  to be on the conservative side. When combining from different measurements, we take the weighted average. For the data which only presented as upper bounds, we assume them to obey Gaussian distribution and taking the error  $\sigma$  accordingly.

The  $\chi^2$  analysis in this case is to minimize the  $\chi^2$  given in the below

$$\chi^2 = \sum_i \frac{(\hat{Br}(i) - Br(i))^2}{\sigma_{Br}^2(i)} + \sum_i \frac{(\hat{A}_{CP}(i) - A_{CP}(i))^2}{\sigma_{CP}^2(i)} + \chi^2(A, |V_{ub}/V_{cb}|), \quad (38)$$

where the summation on  $i$  is for the available decay branching ratios and CP asymmetries listed in Table III.  $\sigma_{Br,CP}$  are the corresponding errors. Here  $\chi^2(A, |V_{ub}/V_{cb}|)$  is the  $\chi^2$  due to uncertainties in  $A$  and  $|V_{ub}/V_{cb}|$  as in section II. The branching ratios  $Br(i)$  and CP asymmetries  $A_{CP}(i)$  expressed in terms of decay amplitude  $A(i) = (G_F/\sqrt{2})[V_{ub}V_{uq}^*T(i) + V_{tb}V_{tq}^*P(i)]$  for a particular  $B \rightarrow P_1P_2$  are given by

$$\begin{aligned} Br(i) &= \frac{1}{32\pi m_B \Gamma_B} (|A(i)|^2 + |\bar{A}(i)|^2) \lambda_{P_1P_2}, \\ A_{CP}(i) &= \frac{|A(i)|^2 - |\bar{A}(i)|^2}{|A(i)|^2 + |\bar{A}(i)|^2}, \end{aligned} \quad (39)$$

where  $\lambda_{ij} = [(1 - (m_i + m_j)^2/m_B^2)(1 - (m_i - m_j)^2/m_B^2)]^{1/2}$ . The amplitudes  $T(i)$  and  $P(i)$  for each individual decay can be read off from Table II.

TABLE III. Rare hadronic charmless  $B \rightarrow \pi\pi$  and  $B \rightarrow K\pi$  data. The branching ratios are in unit of  $10^{-6}$ .

Br and $A_{CP}$	Data	Value used from combined data
$Br(B \rightarrow \pi^+\pi^-)$	$4.3^{+1.6}_{-1.4} \pm 0.5$ [7,28]	$4.4 \pm 0.9$
	$5.9^{+2.4}_{-2.1} \pm 0.5$ [29]	
	$4.1 \pm 1.0 \pm 0.7$ [30]	
$Br(B \rightarrow \pi^-\pi^0)$	$5.6^{+2.6}_{-2.3} \pm 1.7$ [7,28]	$6.2 \pm 2.4$
	$7.1^{+3.6+0.9}_{-3.0-1.2}$ [29]	
$Br(B \rightarrow K^+\pi^-)$	$17.2^{+2.5}_{-2.4} \pm 1.2$ [7,28]	$17.3 \pm 1.6$
	$18.7^{+3.3}_{-3.0} \pm 1.6$ [29]	
	$16.7 \pm 1.6^{+1.2}_{-1.7}$ [30]	
$Br(B \rightarrow K^-\pi^0)$	$11.6^{+3.0+1.4}_{-2.7-1.3}$ [7,28]	$13.7 \pm 2.6$
	$17.0^{+3.7+2.0}_{-3.0-2.2}$ [29]	
$Br(B \rightarrow \bar{K}^0\pi^-)$	$18.2^{+4.6}_{-4.0} \pm 1.6$ [7,28]	$16.2 \pm 3.8$
	$13.1^{+5.5}_{-4.6} \pm 2.6$ [29]	
$Br(B \rightarrow K^0\pi^0)$	$14.6^{+5.9+2.4}_{-5.1-3.3}$ [7,28]	$14.6 \pm 4.6$
	$14.6^{+6.1}_{-5.1} \pm 2.7$ [29]	
$Br(B \rightarrow K^-K^0)$	$< 5.1(90\%C.L.)$ [7,28]	$0.6 \pm 1.9$
	$< 5.0(90\%C.L.)$ [29]	
$Br(B \rightarrow \pi^0\pi^0)$	$2.1^{+1.7+0.7}_{-1.3-0.6}$ [28]	$2.1 \pm 1.8$
$A_{CP}(B \rightarrow K^-\pi^0)$	$-0.29 \pm 0.23$ [31]	$-0.13 \pm 0.16$
	$0.019^{+0.219}_{-0.191}$ [29]	
$A_{CP}(B \rightarrow K^+\pi^-)$	$-0.04 \pm 0.16$ [31]	$-0.003 \pm 0.12$
	$0.043 \pm 0.175 \pm 0.021$ [29]	
$A_{CP}(B \rightarrow \bar{K}^0\pi^-)$	$0.18 \pm 0.24$ [31]	$0.18 \pm 0.24$

We use  $V_{cb} = 0.0402 \pm 0.0019$  and  $|V_{ub}/V_{cb}| = 0.090 \pm 0.025$  in the fitting. The results with exact SU(3) symmetry are shown in Figures 5 and 6 by the solid curves. The best fit values for the hadronic parameters are

$$C_3^P = 0.13, \quad C_3^T = 0.34, \quad C_6^T = 0.13, \quad C_{15}^T = 0.16,$$

$$\delta_{\bar{3}} = -27^\circ, \quad \delta_6 = -20^\circ, \quad \delta_{15} = 35^\circ. \quad (40)$$

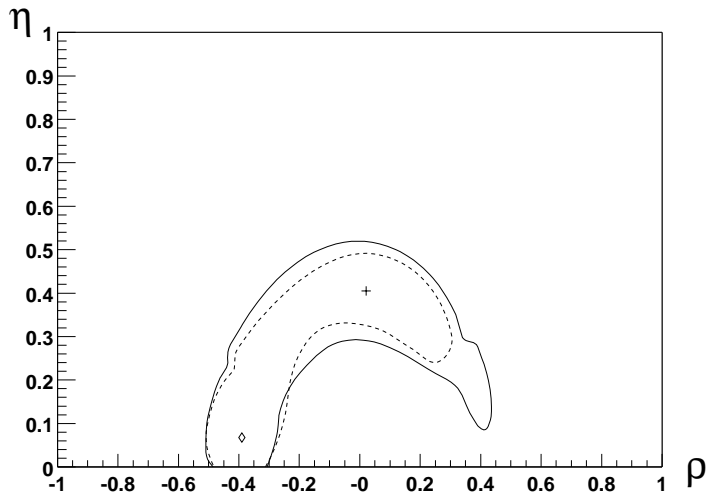


FIG. 5. The constraints for  $\rho$  and  $\eta$  using data from  $|V_{ub}/V_{cb}|$  and rare  $B \rightarrow \pi\pi$  and  $B \rightarrow K\pi$ . For the fit with exact SU(3), the best fit value is indicated by the “+” symbol and the  $\chi^2 - \chi_{min}^2 = 1$  (39% C.L.) allowed regions are inside the region in the solid curve. For the case with SU(3) breaking effects, the best fit value is indicated by a diamond shaped symbol and the 39% C.L. allowed region is inside the dashed curve.

And the best fit values for  $\rho$ ,  $\eta$  and  $\gamma$  are

$$\rho = 0.02, \quad \eta = 0.40, \quad \gamma = 87^\circ. \quad (41)$$

The constraint is weak. We have not given the 68% allowed ranges because to that level, the constraints are basically given by  $|V_{ub}/V_{cb}|$ . We have to wait more accurate data to obtain more restrictive constraints.

At present the errors on the asymmetries are too large and do not really provide stringent constraints. However, we include them here hoping that they will be measured soon. By then one can easily include them in the fit to obtain more stringent constraint on  $\gamma$ .

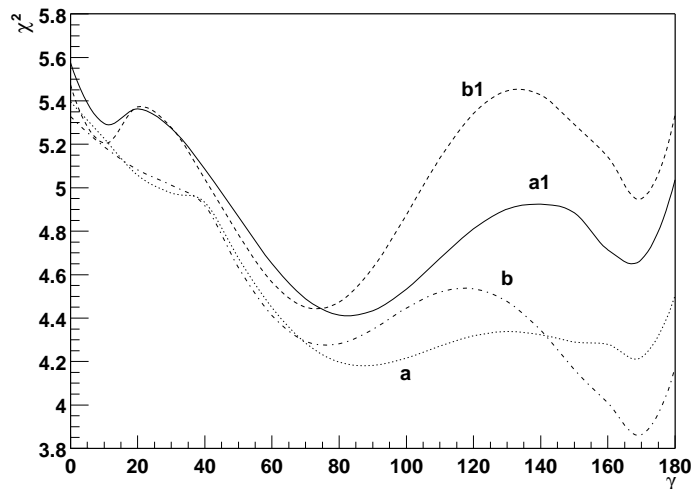


FIG. 6.  $\chi^2$  as a function of  $\gamma$  using data from  $|V_{ub}/V_{cb}|$  and rare  $B \rightarrow \pi\pi$  and  $B \rightarrow K\pi$ . The curve (a) is for the case with exact SU(3), and the curve (b) is for the one with SU(3) breaking effects. The curves (a1) and (b1) are for the cases with the additional condition  $C_3^T e^{i\delta_3} - C_6^T e^{i\delta_6} - C_{15}^T e^{i\delta_{15}} = 0$  with exact SU(3) and with SU(3) breaking effects, respectively.

In Figure 5, we show the regions allowed by  $\chi^2 - \chi_{min}^2 = 1$  in the  $\rho - \eta$  plane by the solid curve. As mentioned that at present the constraint is weak which can also be seen from Figure 6 where the minimal  $\chi^2$  as a function of  $\gamma$  is shown by the curve (a) for the case with exact SU(3) symmetry, although the  $\chi_{min}^2$  per degree of freedom is smaller than 1. The 68% allowed region is actually the same as that from  $|V_{ub}/V_{cb}|$  alone. However, when more precision data for rare charmless  $B \rightarrow PP$  become available, the restriction will become more stringent. For example, if the error bars for all the quantities are reduced by a factor of 2.45, then the regions in Figure 5 correspond to 95% C.L. allowed regions.

SU(3) may not be an exact symmetry for  $B \rightarrow PP$ . We now estimate SU(3) breaking effects. The amplitudes  $C_i$  for  $B \rightarrow \pi\pi$  and  $B \rightarrow K\pi$  will be different if SU(3) is broken. At present it is not possible to calculate the breaking effects. To have some idea about the size of the SU(3) breaking effects, we work with the factorization estimate. To leading order the relation between the amplitudes for  $B \rightarrow \pi\pi$  decays  $C_i(\pi\pi)$  and the amplitudes for  $B \rightarrow K\pi$  decays  $C_i(K\pi)$  can be parameterized as  $C_i(K\pi) = rC_i(\pi\pi)$ , and  $r$  is approximately given

by

$$r \approx \frac{f_K}{f_\pi} = 1.22. \quad (42)$$

Here we have assumed that the SU(3) breaking effects in  $f_i$  and  $F_0^{B \rightarrow i}$  are similar in magnitudes, that is,  $f_K/f_\pi \approx F_0^{B \rightarrow K}/F_0^{B \rightarrow \pi}$  [32]. Using the above to represent SU(3) breaking effect, we can obtain another set of fitting results. They are shown in Figures 5 (dashed curve) and 6 (curve (b)). The best fit values for the amplitudes are

$$\begin{aligned} C_3^P &= 0.11, \quad C_3^T = 0.33, \quad C_6^T = 0.22, \quad C_{15}^T = 0.18, \\ \delta_3 &= 57^\circ, \quad \delta_6 = 200^\circ, \quad \delta_{15} = 85^\circ. \end{aligned} \quad (43)$$

The best fit values for  $\rho$ ,  $\eta$  and  $\gamma$  are given by

$$\rho = -0.39, \quad \eta = 0.07, \quad \gamma = 170^\circ. \quad (44)$$

In both exact and broken SU(3) cases, there are two local minimal in the  $\chi^2$  vs.  $\gamma$  diagrams. The corresponding values of  $\gamma$  are very different with one of them around  $87^\circ$  and another  $170^\circ$ . These best fit values are dramatically different that those obtained in section II. However the best fit values here can not be taken too seriously because, as can be seen from Fig. 5, that at 39% C.L. level, almost all allowed range by  $|V_{ub}/V_{cb}|$  is allowed by  $B \rightarrow PP$  data. At 68% C.L. level, all allowed region by  $|V_{ub}/V_{cb}|$  is allowed by data from  $B \rightarrow PP$  decays. Inconsistence between  $\gamma$  obtained in Section II and this section can not be established. We have to wait more precise data on  $B \rightarrow PP$  to decide.

In the literature it has often been quoted that  $O_{1,2}$  do not contribute to  $B^- \rightarrow \bar{K}^0 \pi^-$  and therefore  $Br(B^- \rightarrow \bar{K}^0 \pi^-) = Br(B^+ \rightarrow K^0 \pi^+)$ . In the SU(3) language used here, this implies  $C = C_3^T e^{i\delta_3} - C_6^T e^{i\delta_6} - C_{15}^T e^{i\delta_{15}} = 0$ . This result has been used to derive several methods to determine the phase  $\gamma$ . We stress that this is not a result from SU(3) consideration and need to be checked. For this reason we also carried out analyses with the condition  $C = 0$ . For this case, the minimal  $\chi^2$  as a function of  $\gamma$  are also shown in Figure 6 (curves (a1) and (b1)) with exact SU(3) and with SU(3) breaking effects, respectively. The best fit values with exact SU(3) symmetry are

$$\begin{aligned}
\rho &= 0.05, \quad \eta = 0.41, \quad \gamma = 83^\circ, \\
C_3^P &= 0.13, \quad C_3^T = 0.26, \quad C_6^T = 0.17, \quad C_{15}^T = 0.16, \\
\delta_{\bar{3}} &= -13^\circ, \quad \delta_6 = -49^\circ, \quad \delta_{15} = 27^\circ.
\end{aligned} \tag{45}$$

And the best fit values with SU(3) breaking effects are

$$\begin{aligned}
\rho &= 0.12, \quad \eta = 0.39, \quad \gamma = 73^\circ, \\
C_3^P &= 0.11, \quad C_3^T = 0.24, \quad C_6^T = 0.15, \quad C_{15}^T = 0.16, \\
\delta_{\bar{3}} &= -15^\circ, \quad \delta_6 = -56^\circ, \quad \delta_{15} = 23^\circ.
\end{aligned} \tag{46}$$

The imposition of  $C = 0$  does not force these coefficients to be real. In order to get  $C$  to be zero, the real and imaginary parts both have to cancel to satisfy the condition. The implications of this analysis will be discussed later.

#### IV. COMBINED FIT

In this section we carry out a combined fit of the sections II and III. The total  $\chi^2(total)$  is the sum of the  $\chi^2(II)$  with  $\sin 2\beta$  data included from section II plus the  $\chi^2(III)$ . Here  $\chi^2(III)$  is the  $\chi^2$  in Eq. (36) of section III with  $\chi^2(A, |V_{ub}/V_{cb}|)$  subtracted. This is because that  $\chi^2(II)$  already included information from  $A$  and  $|V_{ub}/V_{cb}|$ . The results are shown in Figures 7 and 8. Since  $\chi^2(II)$  has a sharper dependence on  $\gamma$  compared with  $\chi^2(III)$ , the best fit values and errors are dominantly determined by constraints in section II.

The best combined fit values with exact SU(3) symmetry for the hadronic parameters are

$$\begin{aligned}
C_3^P &= 0.13, \quad C_3^T = 0.29, \quad C_6^T = 0.16, \quad C_{15}^T = 0.20, \\
\delta_{\bar{3}} &= -42^\circ, \quad \delta_6 = -20^\circ, \quad \delta_{15} = 35^\circ.
\end{aligned} \tag{47}$$

In the above we have not given errors for the hadronic parameters because the constraints on them are weak.



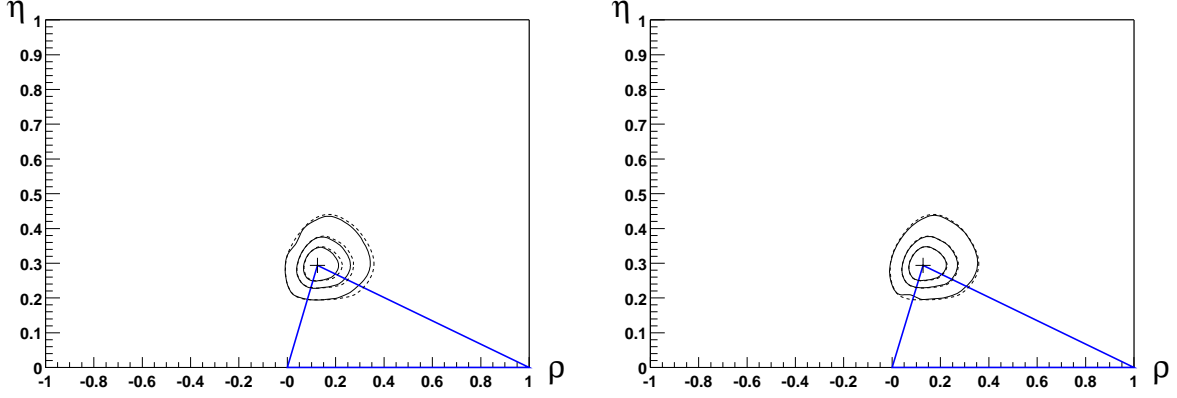


FIG. 7. Constraints on  $\rho$  and  $\eta$  using combined data from  $|\epsilon_K|$ ,  $\Delta m_{B_{d,s}}$ ,  $|V_{ub}/V_{cb}|$ ,  $\sin 2\beta$  and  $B \rightarrow \pi\pi$  and  $B \rightarrow K\pi$ . The three regions from smaller to larger corresponds to  $\chi^2 - \chi_{min}^2 = 1$  allowed region which is at the 39% C.L., the 68% C.L. allowed region and the 95% C.L. allowed region, respectively. The figure on the left is for the case with exact SU(3) and the one on the right is for the case with SU(3) breaking effects. The dotted curves are for fit in section II and the solid curves are for the combined fit.

The best fit values for  $\rho$ ,  $\eta$  and  $\gamma$  and their 68% C.L. errors are given by

$$\rho = 0.12_{-0.05}^{+0.09}, \quad \eta = 0.29_{-0.04}^{+0.06}, \quad \gamma = 67_{-13}^{+10}, \quad (48)$$

and the 95% C.L. allowed ranges for  $\rho$ ,  $\eta$  and  $\gamma$  are

$$\begin{aligned} 0.01 < \rho < 0.29, \quad 0.21 < \eta < 0.40, \\ -0.86 < \sin 2\alpha < 0.45, \quad 0.45 < \sin 2\beta < 0.79, \quad 43^\circ < \gamma < 87^\circ. \end{aligned} \quad (49)$$

The best combined fit values with SU(3) breaking effects for the hadronic parameters are

$$\begin{aligned} C_3^P &= 0.11, \quad C_3^T = 0.29, \quad C_6^T = 0.16, \quad C_{15}^T = 0.20, \\ \delta_3 &= -33^\circ, \quad \delta_6 = -40^\circ, \quad \delta_{15} = 31^\circ. \end{aligned} \quad (50)$$

$$\rho = 0.13_{-0.06}^{+0.09}, \quad \eta = 0.29_{-0.04}^{+0.06}, \quad \gamma = 66_{-13}^{+10}, \quad (51)$$

and the 95% C.L. allowed ranges for  $\rho$ ,  $\eta$  and  $\gamma$  are

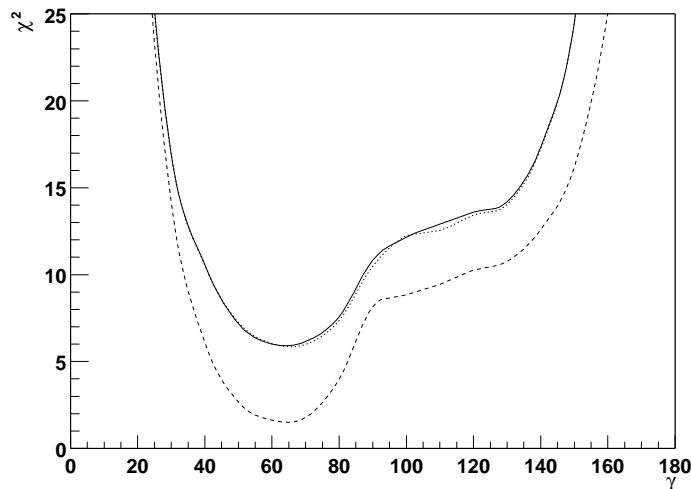


FIG. 8.  $\chi^2$  as a function of  $\gamma$  using combined data from  $|\epsilon_K|$ ,  $\Delta m_{B_{d,s}}$ ,  $|V_{ub}/V_{cb}|$ ,  $\sin 2\beta$  and rare  $B \rightarrow PP$  data. The dotted and solid curves are for the fit with exact SU(3) and with SU(3) breaking effects, respectively. The dashed curve is the same as that from section II with  $\sin 2\beta$  included.

$$\begin{aligned}
 0.01 < \rho < 0.30, \quad 0.21 < \eta < 0.41, \\
 -0.87 < \sin 2\alpha < 0.44, \quad 0.46 < \sin 2\beta < 0.80, \quad 42^\circ < \gamma < 87^\circ.
 \end{aligned}
 \tag{52}$$

## V. DISCUSSIONS AND CONCLUSIONS

At present the rare charmless hadronic  $B$  decay data have large error bars. The main contribution to the  $\chi^2$  for the analysis in sections III and IV come from the branching ratio for  $\bar{B}^0 \rightarrow \bar{K}^0 \pi^0$ . In the cases discussed, this mode alone contribute about 2.5 to the  $\chi^2$ . The best fit value of the branching ratio is only about half of the experimental central value. We suspect that there may be some systematic errors in the measurement of this branching ratio. If the present central value persists, it may be an indication of badly broken SU(3) symmetry or new physics beyond the SM. It is important to improve the precision of experimental data to decide whether new physics is needed.

Because of the large error bars associated with the  $B \rightarrow PP$  data, the ranges determined for the related parameters have large error bars. Especially the phase  $\gamma$  has a large range

allowed using the  $B \rightarrow PP$  data alone. However, the fit shows no conflict between the fit from the consideration using  $|\epsilon_K|$ ,  $\Delta m_{B_{d,s}}$ ,  $|V_{ub}/V_{cb}|$  and  $\sin 2\beta$  data. Future experimental data will be able to provide a more accurate determination of the phase  $\gamma$ .

Before closing we would like to make a few comments about our analysis and some other related calculations. Our first comment concerns the general SU(3) analysis and factorization calculations.

Assuming factorization and SU(3) symmetry, that is the decay constants for all octet pseudoscalars  $P$  are equal, and the form factors for  $B \rightarrow P$  are also equal, one obtains [26]

$$\begin{aligned} C_3^T &= \left\{ \frac{3a_2 - a_1}{8} - [(a_4^{uc} + a_6^{uc}R) + \frac{3}{16}(a_7^{uc} - a_9^{uc}) + \frac{1}{16}(a_{10}^{uc} + a_8^{uc}R)] \right\} X \\ C_6^T &= \left\{ \frac{a_2 - a_1}{4} - \frac{3}{8}(a_{10}^{uc} - a_9^{uc} + a_7^{uc} + a_8^{uc}R) \right\} X \\ C_{15}^T &= \left\{ \frac{a_1 + a_2}{8} - \frac{3}{16}(a_9^{uc} + a_{10}^{uc} - a_7^{uc} + a_8^{uc}R) \right\} X \end{aligned} \quad (53)$$

where  $X = f_\pi F_0^{B \rightarrow \pi}(m_\pi^2)(m_B^2 - m_\pi^2)$  and  $R = m_K^2/(m_b - m_q)(m_s + m_q)$ . These amplitudes are related to the ‘‘tree’’ contributions,  $a_i^{uc} = a_i^u - a_i^c$  with  $a_{2i} = c_{2i} + c_{2i-1}/N$  and  $a_{2i-1} = c_{2i-1} + c_{2i}/N$ .

The penguin amplitudes are given by [26]

$$\begin{aligned} C_3^P &= -[(a_4^{tc} + a_6^{tc}R) + \frac{3}{16}(a_7^{tc} - a_9^{tc}) + \frac{1}{16}(a_{10}^{tc} + a_8^{tc}R)] X, \\ C_6^P &= -\frac{3}{8}(a_{10}^{tc} - a_9^{tc} + a_7^{tc} + a_8^{tc}R) X, \\ C_{15}^P &= -\frac{3}{16}(a_9^{tc} + a_{10}^{tc} - a_7^{tc} + a_8^{tc}R) X. \end{aligned} \quad (54)$$

where  $a_i^{tc} = a_i^t - a_i^c$ . When small contributions from  $a_{7,8}^{ij}$  terms are neglected, one recovers the relations in Eq. (36). Numerically, we have

$$\begin{aligned} C_3^P &= 0.09, \quad C_3^T = 0.42, \quad C_6^T = 0.26, \quad C_{15}^T = 0.15, \\ \delta_3 &= -15.7^\circ, \quad \delta_6 = -14.5^\circ, \quad \delta_{15} = -14.5^\circ. \end{aligned} \quad (55)$$

In the above we have used the convention with  $C_3^P$  to be real.

The amplitudes are in the same order of magnitude as the best fit values in sections III and IV, but the phase can be very different. In the factorization approximation calculation

here, phases are only due to short distance interaction, rescattering of quarks. Long distance contributions can change these phases. The results of the best fit values for the phases indicating that there may be large long distance rescattering effects.

Our second comments concerns the combination of the SU(3) invariant decay amplitude  $C = C_3^T e^{i\delta_3} - C_6^T e^{i\delta_6} - C_{15}^T e^{i\delta_{15}}$ . It has been usually assumed that in the literature that  $C = 0$ . This leads to  $Br(B^+ \rightarrow K^0 \pi^+) = Br(B^- \rightarrow \bar{K}^0 \pi^-)$ . This result played a crucial role in several methods to constrain and to determine the phase  $\gamma$ , for example, using [9]  $B^- \rightarrow K^- \pi^0, \bar{K}^0 \pi^-, \pi^- \pi^-, \bar{B}^0(B^-) \rightarrow K^+ \pi^-, \pi^+ \pi^-(\bar{K}^0 \pi^-)$ , and  $B^- \rightarrow K^- \pi^0, \bar{K}^0 \pi^-, K^- \eta$ .

We point out that  $C = 0$  is based on factorization calculation neglecting annihilation contributions and also penguin contributions [26]. In fact, using factorization calculation when penguin contributions are included,  $C$  does not equal to zero, but  $C = C_3^T(penguin)$ .  $C_3^T(penguin)$  can be obtained from Eq.(53) (the terms proportional to  $c_i^{uc}$  in  $C_3^T$ ). In the factorization framework, we can easily check whether  $C = 0$  is a good approximation. Using the result in Eq. (53) we find that the  $|C_3^T(penguin)/C_3^T|$  is of order 5%. It is therefore reasonable to assume the penguin contribution to be small and  $C \approx 0$ .

One should also be aware that when going beyond factorization approximation and include rescattering effects  $C$  may deviate from zero. It should be tested. The fitting program proposed in this paper can be easily used to achieve this goal. From the best fit values in the previous sections, we clearly see that  $C$  can easily deviate from zero. For example, in the case with exact SU(3), the best fit value using rare  $B$  decay data  $C$  is,  $C = 0.05 - i0.20$  and with SU(3) breaking effects  $C$  is,  $C = 0.37 + i0.18$  which are the same order of magnitude as individual  $C_i^T$ . One needs more data to achieve a better test. Until then, the use of the methods based on the above equation have to be treated with caution.

Our final comments concerns the uncertainties in the present analysis. In this paper we have developed a method based on SU(3) flavor symmetry to determine the CP violating phase  $\gamma$ . We find that when annihilation contributions are neglected, there are only seven hadronic parameters in the SM related to  $B \rightarrow PP$  decays. The annihilation contributions are small is based on factorization approximation. If it turns out that they are not small,

as some model calculations indicated that the penguin related annihilation contribution  $A_3^P$  may be sizeable, one needs to include it into the analysis. However, from Table II one can see that  $A_3^P$  does not show up in  $B \rightarrow K\pi$  decays, but only to  $B \rightarrow \pi\pi$  which is suppressed by small Wilson coefficients. One can also carried out an analysis including  $A_3^P$  into the fit when more experimental data become available. Future experimental data with better accuracy will provide more information.

In the estimate of SU(3) breaking effects, we have parameterized the SU(3) breaking effects in a simple form with  $C_i(K\pi) = (f_K/f_\pi)C_i(\pi\pi)$ . In general the SU(3) breaking effects may be more complicated. More systematic study of SU(3) breaking effects are needed in order to obtain more accurate determination of the phase  $\gamma$ . But in any rate we hope that the method developed here will help to provide useful information about the hadronic matrix elements and also the CP violating phase  $\gamma$ .

In conclusion, in this paper we have developed a method to determine the CP violating phase  $\gamma$  based on the flavor SU(3) symmetry. We find that present data can already give some constraint on  $\gamma$  and it is consistent with the constraint obtained by using  $|\epsilon_K|$ ,  $\Delta m_{B_{d,s}}$ ,  $|V_{ub}/V_{cb}|$  and  $\sin 2\beta$  data. We also carried out an analysis combining data from  $\epsilon_K$ ,  $\Delta m_{B_{d,s}}$ ,  $|V_{ub}/V_{cb}|$ ,  $\sin 2\beta$  and data from rare charmless hadronic  $B$  decays. The combined analysis gives  $\gamma = 67^\circ$  for the best fit value and  $43^\circ \sim 87^\circ$  as the 95% C.L. allowed range. Although there are uncertainties in the fit program, the method developed in the present paper can provide useful information about the hadronic matrix elements for rare charmless hadronic B decays and the CP violating phase  $\gamma$ .

XGH would like to thank P. Chang and D. London for useful discussions. XGH, YKH and JQS were supported by the National Science Council of ROC under grant number NSC89-2112-M-002-058 and NCTS of ROC, and, YLW and YFZ were supported by the NSF of China under the grant No. 19625514.

## REFERENCES

- [1] M. Kobayashi and T. Maskawa, Prog. Theor. Phys. **49**, 652(1973).
- [2] N. Cabibbo, Phys. Rev. Lett. **10**, 531(1963).
- [3] Particle Data Group, Eur. Phys. J. **C 15** 1(2000).
- [4] L. Wolfenstein, Phys. Rev. Lett. **51**, 1945(1983).
- [5] S. Mele, Phys.Rev. **D59** 113011(1999); A. Ali, D. London, Eur.Phys.J. **C9** 687(1999).
- [6] F. Parodi, P. Roudeau and A. Stocchi, Nuovo. Cim. **A112**, 833(1999); F. Caravaglios et al., e-print hep-ph/0002171.
- [7] CLEO Collaboration, D. Cronin-Hennessy et al., Phys. Rev. Lett.**85**, 525(2000).
- [8] N. G. Deshpande, et al., Phys. Rev. Lett. **82** 2240(1999); X.-G. He, W.-S. Hou and K.-C. Yang, Phys. Rev. Lett. **83**, 1100(1999); W.-S. Hou, J. G. Smith, F. Wurthwein, e-print hep-ex/9910014; C. Isola and T.N. Pham, e-print hep-ph/0009210; Y-L. Wu and Y.-F. Zhou, Phys. Rev. **D62**, 036007(2000); A. Buras and R. Fleischer, Eur. Phys. J. **C16**, 97(2000); M. Beneke et al., e-print hep-ph/0007256; Y.-Y. Keum, H.-n. Li and A.I. Sanda, e-print hep-ph/0004004.
- [9] R. Fleischer and T. Mannel, Phys. Rev. **D57**, 2752(1998); M. Neubert and J. Rosner, Phys. Lett. **B441**, 403(1998); M. Neubert and J. Rosner, Phys. Rev. Lett. **81**, 5076(1998); X.-G. He, C.-L. Hsueh and J.-Q. Shi, Phys. Rev. Lett. **84** 18(2000); M. Gronau and J. Rosner, Phys. Rev. **D57**, 6843(1998); N.G. Deshpande and X.-G. He, Phys. Rev. Lett. **75**, 3064(1995).
- [10] M. Savage and M. Wise, Phys. Rev. **D39**, 3346(1989); *ibid* **D40**, Erratum, 3127(1989); X.-G. He, Eur. Phys. J. **C9**, 443(1999); N. G. Deshpande, X.-G. He, and J.-Q. Shi, Phys. Rev. **D62**, 034018(2000).
- [11] M. Gronau et al., Phys. Rev. **D50**, 4529 (1994); **D52**, 6356 (1995); *ibid*, 6374 (1995);

- A.S. Dighe, M. Gronau and J. Rosner, Phys. Rev. Lett. **79**, 4333 (1997); L.L. Chau et al., Phys. Rev. **D43**, 2176 (1991); D. Zeppendfeld, Z. Phys. **C8**, 77(1981).
- [12] M. Gronau and D. London, Phys. Rev. Lett. **65**, 3381(1990); N. G. Deshpande and X.-G. He, Phys. Rev. Lett. **75**, 1703(1995); M. Gronau and J. Rosner, Phys. Rev. **D57**, 6843(1998); *ibid*, **D61**, 073008(2000); Phys. Lett. **B482**, 71(2000), M. Gronau, D. Pirjol and T.-M. Yan, Phys. Rev. **D60**, 034021(1999).
- [13] X.-G. He, J.-Y. Leou and C.-Y. Wu, Phys. Rev. **D62**, 114015(2000).
- [14] Y.-F. Zhou et al., e-print hep-ph/0006225 (in press in Phys. Rev. D).
- [15] S. Herrlich and U. Nierste, Nucl. Phys.**B 419**, 292(1994); A. J. Buras, M. Jamin and P.H. Weisz, Nucl. Phys. **B 347**, 491(1990); S. Herrlich and U. Nierste, Phys. Rev. **D 52**, 6505(1995).
- [16] T. Draper, e-print hep-lat/9810065, Nucl. Phys. Proc. Suppl. **73**, 43(1999); S. Sharpe, e-print hep-lat/9811006; JLQCD Collab., S. Aoki et al., Nucl. Phys. B (proc. Suppl) **63A-C** 281(1998).
- [17] A. Ali and D. London, Z. Phys. **C 65** 431(1995); Takeo Inami, C.S. Lim, B. Takeuchi, M. Tanabashi, Phys. Lett. **B381** 458(1996).
- [18] The LEP B oscillation WG, <http://lepbosec.web.cern.ch/LEPBOSC>, updated for XXXth International Conference on High Energy Physics, Osaka, Japan.
- [19] J. M. Flynn, C. T. Sachrajda, hep-lat/9710057, to appear in Heavy Flavours (2nd edition) edited by A J Buras and M Lindner (World Scientific, Singapore).
- [20] H. G. Moser and A. Roussani, Nucl. Inst. Meth. **A384**, 491(1997).
- [21] The BABAR Collaboration, B. Aubert, et al, submitted to P.R.L. A. Abashian et al. (Belle Collaboration), submitted to P.R.L.
- [22] T. Affolder et al. (CDF Collaboration), Phys. Rev. **D61** 072205(2000).

- [23] The ALEPH Collaboration, e-print hep-ex/0009058, Phys. Lett. **492**, 259(2000).
- [24] G. Buchalla, A. Buras and M.Lautenbacher, Rev. Mod. Phys. **68**, 1125(1996);  
M.Ciuchini et.al., Nucl. Phys. **B415**, 403(1994).
- [25] N. G. Deshpande and X.-G. He, Phys. Lett. **B336**, 471 (1994).
- [26] A. Ali, G. Kramer and C.-D. Lu, Phys. Rev. **D58**, 094009(1998); *ibid* **D59** 014005(1999);  
A. Datta, X.-G. He and S. Pakvasa, Phys. Lett. **B419**, 369(1998); Y.-H. Chen, H.-Y.  
Cheng, B. Tseng, K.-C. Yang, Phys. Rev. **D60** 094014(1999).
- [27] R. Fleischer, Z. Phys. **C62**, 81(1994); Phys. Lett. **B321**, 259(1994); Phys. Lett. **B332**,  
419(1994); N. Deshpande, X.-G. He and J. Trampetic, Phys. Lett. **B345**, 547 (1995);  
N.G. Deshpande and X.-G. He, Phys. Rev. Lett. **74**, 26 (1995); 4099(E) (1995).
- [28] D. Urner, CLEO TALK 00-33, DPF2000, Columbus, Ohio, USA, August 9-12, 2000; R.  
Stroynowshi, CLEO Talk 00-30, ICHEP2000, Osaka, Japan, July 27 to August 2, 2000.
- [29] T. Iijima, Belle Collaboration, Talk at BCP4, Ise-Shima, Japan, February 19-23, 2001.
- [30] A. Hoecker, Paris-Sud , Babar Collaboration, Talk at BCP4, Ise-Shima, Japan, February  
19-23, 2001.
- [31] CLEO Collaboration, S. Chen et al., Phys. Rev. Lett.**85**, 525(2000).
- [32] D. Melikhov and B. Stech, Phys. Rev. **D62**, 014006(2000).